Published in final edited form as:
Sci Transl Med. 2011 November 23; 3(110): 110ra118. doi:10.1126/scitranslmed.3003126.

Bactericidal/permeability-increasing protein ($rBPI_{21}$) and fluoroquinolone mitigate radiation-induced bone marrow aplasia and death

Eva C. Guinan[1,2,11,12], **Christine M. Barbon**[3], **Leslie A. Kalish**[6], **Kalindi Parmar**[1], **Jeff Kutok**[8,#], **Christy J. Mancuso**[5], **Liat Stoler-Barak**[5,##], **Eugénie E. Suter**[5,###], **Janice D. Russell**[1], **Christine D. Palmer**[5], **Leighanne C. Gallington**[5,####], **Annie Voskertchian**[3], **Jo-Anne Vergilio**[7], **Geoffrey Cole**[3], **Kaya Zhu**[1], **Alan D'Andrea**[1], **Robert Soiffer**[3,13], **Jerrold P. Weiss**[9], and **Ofer Levy**[5,10,12]

[1]Department of Radiation Oncology, Dana-Farber Cancer Institute, Boston, MA 02215, USA

[2]Department of Pediatrics, Dana-Farber Cancer Institute, Boston, MA 02215, USA

[3]Department of Medical Oncology, Dana-Farber Cancer Institute, Boston, MA 02215, USA

[4]Division of Hematology/Oncology, Children's Hospital Boston, Boston, MA 02115, USA

[5]Division of Infectious Diseases, Children's Hospital Boston, Boston, MA 02115, USA

[6]Division of Clinical Research Program, Children's Hospital Boston, Boston, MA 02115, USA

[7]Department of Pathology, Children's Hospital Boston, Boston, MA 02115, USA

Corresponding Author. Eva C. Guinan MD, Dana-Farber Cancer Institute, 450 Brookline Avenue, Boston, MA USA 02215, Phone: 617-632-4932, FAX: 617-632-3770, eva_guinan@dfci.harvard.edu.
[#]Present address:
Infinity Pharmaceuticals, 780 Memorial Drive, Cambridge, MA, USA02139
[##]The Weizmann Institute, Rehovot, 76100, Israel.
[###]Feinberg School of Medicine, Northwestern University, 420 East Superior Street Chicago, IL, USA 60611
[####]Georgia Institute of Technology; Atlanta, GA, USA 30332

List of Supplementary Material

Tables

S1. Characteristics and treatment of patients undergoing myeloablative transplantation on the observational cohort study.
S2. Median fold-difference in peripheral blood levels of chemokines and cytokines after radiation alone, radiation with indicated treatment, or no irradiation.

Figures

S1. 7 Gy irradiation of BALB/c mice is associated with subsequent endotoxemia.
S2. Effect of $rBPI_{21}$/ENR and VEH/ENR on survival is reproducible.
S3. $rBPI_{21}$/ENR does not mitigate early GI damage after 7 Gy irradiation.
S4. Trilineage hematopoiesisis is evident in bone marrow of treated mice.
S5. Effects of 14 and 30 days of $rBPI_{21}$ plus ENR on bone marrow mononuclear cell, LSK and LK cells are equivalent.
S6. Effects of 14 and 30 days of $rBPI_{21}$ plus ENR on peripheral blood counts are equivalent.
S7. Gating strategy for determining LK and LSK cells in bone marrow from BALB/c mice by flow cytometry.

Author contributions: ECG and OL conceived the studies, executed the clinical study, designed experiments, analyzed and interpreted data, and drafted the article. CMB designed experiments, developed methods, performed experiments, data analysis, and drafted and reviewed the manuscript. LK analyzed and interpreted data and provided critical manuscript revision. JK and J-AV analyzed murine data and reviewed the manuscript. KP contributed to initial murine experimental design, data interpretation, and manuscript review. AD provided important resources for murine studies and reviewed the manuscript. GC performed experiments and manuscript review. ES, LS-B, CP, CM, JDR, LCG, KZ and AV contributed to experiment planning, execution, analysis, and manuscript preparation. RS contributed to human study execution and manuscript review. JW reviewed and interpreted data and contributed critical manuscript revisions.

Competing interests: OL's laboratory received sponsorship and reagent support from XOMA (US) LLC and Spectral Diagnostics.

[8]Department of Pathology, Brigham and Women's Hospital, Boston MA 02115, USA

[9]Inflammation Program and Department of Medicine, University of Iowa, Coralville, IA 52241, USA

[10]Leder Human Biology and Translational Medicine Program, Harvard Medical School, Boston, MA, 02115, USA

[11]Department of Radiation Oncology, Harvard Medical School, Boston, MA, 02115, USA

[12]Department of Pediatrics, Harvard Medical School, Boston, MA, 02115, USA

[13]Department of Medicine, Harvard Medical School, Boston, MA, 02115, USA

Abstract

Identification of safe, effective treatment strategies to mitigate toxicity after extensive radiation exposure has proven challenging. Only a limited number of candidate approaches have emerged, and the Federal Drug Administration has yet to approve any agent for a mass-casualty radiation disaster indication. As preparative treatments for hematopoietic stem cell transplantation (HSCT) produce toxicities similar to such radiation exposures, we studied patients early after myeloablative HSCT to identify new approaches to this problem. Patients rapidly developed endotoxemia and reduced plasma bactericidal/permeability-increasing protein (BPI), a potent endotoxin-neutralizing protein, in association with neutropenia. We hypothesized that a treatment supplying similar endotoxin-neutralizing activity might replace the BPI deficit and mitigate radiation toxicity. We tested this idea in mice. A single 7 Gy radiation dose, which was 95% lethal by 30 days, was followed 24 hours later by twice daily subcutaneous injections of the recombinant BPI fragment $rBPI_{21}$ or vehicle alone for 14 or 30 days, with or without an oral fluoroquinolone antibiotic with broad-spectrum anti-bacterial activity including that against endotoxin-bearing Gram-negative bacteria. Compared to either fluoroquinolone alone or vehicle/fluoroquinolone, combined $rBPI_{21}$/fluoroquinolone treatment improved survival, accelerated hematopoietic recovery and promoted expansion of stem and progenitor cells. The observed efficacy of $rBPI_{21}$ and fluoroquinolones initiated 24 hours after lethal irradiation, combined with their favorable bioactivity and safety profiles in critically-ill humans, suggest the potential clinical utility of this radiation mitigation strategy and support its further evaluation.

Introduction

The U.S. Congress appropriated funds to create a therapeutics stockpile to counter biological and chemical threats in 1988. Subsequently reconfigured as the Strategic National Stockpile (SNS) and managed by the Department of Health and Human Services, SNS is a "national repository of antibiotics, chemical antidotes, antitoxins, life-support medications…designed to supplement and resupply state and local public health agencies in the event of a national emergency anywhere and at anytime" (1). Such an emergency may arise from a nuclear event, which, as Chernobyl and Fukushima demonstrate, can present enormous challenges even without detonation-related toxicities. Rapid exposure of extensive body surface area to significant doses of penetrating radiation results in acute radiation syndrome (ARS) (2–4). ARS, which can affect the hematopoietic, gastrointestinal (GI), central nervous and

cardiovascular systems, can manifest within minutes and last for weeks. To date, only five agents in the SNS address radiation exposure. Three are intended to promote clearance of internal radiation: calcium and zinc DTPA (chelating agents for the transuranium elements plutonium, americium and curium) and Prussian blue (an ion exchanger for cesium-137 and thallium-201). The fourth, potassium iodide, blocks thyroid uptake of radioactive iodine. Only one agent, G-CSF (granulocyte colony-stimulating factor), used to stimulate hematopoietic recovery after intensive cancer treatment, has the potential to mitigate toxicity after radiation exposure, as inferred from human cancer therapy and animal radiation models (5,6). G-CSF is not approved for radiation-induced neutropenia and can be obtained from SNS only with Emergency Use Authorization under an Investigational New Drug application (1).

In humans and mice, both radiation dose and host characteristics determine the extent of injury after exposure. At doses that are frequently fatal within weeks (4–10 Gy), hematopoietic toxicity (hematopoietic syndrome) contributes to mortality as demonstrated by the success of bone marrow shielding, hematopoietic stem cell transplant (HSCT) and G-CSF use in supporting recovery (3,4,6,7). At higher doses, death occurs earlier and even HSCT does not reduce mortality (2–4,6). Concomitant thermal and skin injuries compromise survival at all doses (3,7,8).

Post-radiation bacteremia contributes to total body irradiation (TBI) toxicity (9). Radiation alters both GI mucosal integrity, resulting in translocation of bacteria and bacterial products to the systemic circulation (10,11), and the GI microbiome, favoring predominance of Gram-negative bacteria associated with increased mortality (9). In experimental animal models, administration of antibiotics active against Gram-negative bacteria, including fluoroquinolones, generally reduces radiation-induced mortality, although efficacy varies widely depending upon the model used (9,12). Consistent with a potentially detrimental role of endogenous flora, gnotobiotic (germ-free) mice show better survival than mice with conventional microflora at equivalent radiation dose, survive longer after lethal irradiation, require higher radiation doses to induce GI histopathologic changes, and more effectively repair radiation enteritis (10,13).

Bacteria-derived components that engage the innate immune system influence the sequelae of radiation (10,13–17). Endotoxin, found uniquely in the outer leaflet of the outer membrane of Gram-negative bacteria such as the *Enterobacteriaceae* that colonize the human intestinal tract, translocates into the bloodstream in both bacteriaassociated and free forms after radiation-induced mucosal injury (11). Humans are exquisitely sensitive to even picogram amounts of endotoxin, which promotes activation of host defenses in extravascular tissue but produces cardiovascular and pulmonary instability, dysregulated coagulation and systemic inflammation during endotoxemia. Endotoxin sensitivity can be modified by changes in expression of host endotoxin-recognition proteins that promote either endotoxin activity or detoxification and enhanced clearance of endotoxin (18–20). Of these host proteins, BPI, a 50–55 kDa cationic antimicrobial protein found primarily in the azurophilic granules of human neutrophils, has the highest affinity (pM-nM) for endotoxin (21). Most BPI is intracellular, but plasma concentrations of BPI rise with neutrophil activation and degranulation. BPI binding to endotoxin is anti-infective, promoting killing and

opsonization of Gram-negative bacteria (21). Although conventional antibiotics can kill bacteria, antibiotics do not promote opsonization nor do they mitigate the inflammatory responses induced by cell-free components derived from dead or dying bacteria. As BPI binds both bacteria-associated and cell-free endotoxin, it effectively inhibits endotoxin-induced inflammation and apoptosis by precluding endotoxin ligation of the cellular pro-inflammatory endotoxin receptor complex composed of mCD14, MD-2, and TLR4 (21).

Herein, we demonstrate that humans undergoing myeloablative HSCT become deficient in the endotoxin-neutralizing BPI protein, concurrent with treatment-related endotoxemia. Using a murine model, we then demonstrate that BPI supplementation is an effective radiation mitigation strategy.

Results

Human myeloablative HSCT is associated with early neutropenia, endotoxemia, deficiency of BPI and evidence of host responses to endotoxin

We examined endotoxin and plasma BPI concentrations in an observational cohort study of patients undergoing myeloablative conditioning for HSCT (Table S1). As expected, myeloablative therapy followed by allogeneic HSC infusion resulted in a fall and recovery in peripheral blood counts (Fig. 1A). By the completion of myeloablative conditioning on day 0 (D0), endotoxemia was readily detectable (Fig. 1B). Simultaneously, plasma BPI concentrations declined rapidly (median decrease of 71-fold on day 7, inter-quartile range 9–193-fold; Fig. 1B), correlating with the absolute neutrophil count (ANC; Spearman $r = 0.66$; $p < 0.001$). At the ANC nadir (D7), plasma BPI was undetectable (< 100 pg/mL) in 37/48 patients (77%) and 8 of the 10 patients evaluated by Endotoxin Activity Assay were endotoxemic.

The mCD14 and TLR4 components of the TLR endotoxin receptor on peripheral blood monocytes exhibited increased and decreased surface expression, respectively, on D0 consistent with exposure to bioactive endotoxin (Fig. 1C) (20,21) Subsequent elevation of IL-6 and fever, well–described as frequent sequelae of endotoxemia (22), were maximal at the BPI nadir (D7, Fig. 1D). Intrapatient changes in IL-6 levels were positively correlated with the Endotoxin Activity Assay (Spearman 0.48, $p=0.01$). Higher IL-6 concentrations were inversely correlated with BPI concentrations (Spearman −.30, $p<0.0001$). Although fever and BPI levels showed no association on D7, perhaps because nearly 80% of patients had undetectable BPI, on D14 patients with fever had lower BPI concentrations than afebrile patients (medians: undetectable vs. 3475 pg/mL, $p=0.01$). Notably, lower plasma BPI concentrations on D0, immediately prior to HSC infusion, were associated with slower neutrophil engraftment (Spearman $r=-.33$, $p =0.03$).

These findings suggested that BPI deficiency coupled with endotoxemia could exacerbate endotoxin-related toxicity after myeloablation and impair engraftment, raising the possibility that BPI supplementation might attenuate these toxicities. HSC support is not a readily deployable strategy for mass radiation exposure. As TBI mitigation without HSC cannot be addressed experimentally in humans, we employed a murine model to test our hypothesis.

Characterization of the toxicity of 7 Gy single fraction TBI in BALB/c mice

To model potentially lethal radiation exposure, we defined a dose of single fraction TBI associated with BONE MARROW aplasia, GI damage, and substantial early mortality in BALB/c mice. A single fraction of 7 Gy was associated with 95–100% mortality by D30 ($LD_{95/30}$) in 12 week old male BALB/c (Fig. 2A). The lethality of 7 Gy exposure was highly reproducible: only 5/110 7 Gy irradiated mice (4.5%) survived to D30 and median survival in separate experiments ranged from 12–15 days. After 7 Gy TBI, colonic epithelial apoptosis increased and peaked at D3, and was associated with a parallel fall in plasma citrulline levels, which reflects reduced functional GI enterocyte mass (23) (Fig. 2B). Both GI mucosal parameters improved by D6–9. Endotoxemia was also detectable by D3 and persisted until peaking higher just prior to death (Fig. S1). By D3, the bone marrow was aplastic (Fig. 2C), with an approximate 2 log fall in bone marrow mononuclear cell content, including a decrement in hematopoietic stem (LSK, Lin^- $Sca\text{-}1^+$ *c-Kit*$^+$) and progenitor (LK, Lin^- $Sca\text{-}1^-$ *c-Kit*$^+$) cells (Fig. 2D, E, F).

To ensure the model was adequately myeloablative, we compared the hematopoietic effects of 7 and 6.5 Gy. Despite identical early histologic aplasia, mice had significantly fewer bone marrow mononuclear cells after 7 Gy on D3, 10 and 15 (Fig. 2D). On day 15, LK and LSK cell numbers were significantly lower in the 7 Gy group (Fig. 2E, F). Subsequent experiments were performed with 7 Gy.

rBPI21 and enrofloxacin (ENR) administration markedly decrease TBI-related mortality

The combination ($rBPI_{21}$/ENR) of $rBPI_{21}$ and oral ENR, a veterinary fluoroquinolone antibiotic analogous to ciprofloxacin (24), initiated 24 hours after 7 Gy TBI and continued through D30, significantly improved D30 survival in comparison to VEH/ENR (VEH denotes the formulation buffer for $rBPI_{21}$), ENR and 7 Gy alone (Figs. 3A and S2). Moreover, only 4 deaths of 53 at-risk $rBPI_{21}$/ENR treated mice occurred after D14 whereas losses in the other groups ranged from 38–83% of at-risk animals. Seventeen irradiated, $rBPI_{21}$/ENR treated mice in two separate studies, spaced approximately four months apart, were followed beyond D30. As of D242 and D131, respectively, all are alive and appear healthy. Three irradiated ENR treated mice from the first of the two above studies were also followed past D30. One died at D68 and two healthy appearing mice are still alive at D242.

$rBPI_{21}$ has a 3 hour half-life in mice when administered by intravenous bolus or subcutaneous (SC) injection. As optimal continuous or 6 hour interval IV or SC injection regimens were not feasible, we elected to use twice daily SC administration, initiating all treatments 24 hours after TBI and continuing through D30. As illustrated in Fig. 3A, VEH/ENR, the control for the $rBPI_{21}$/ENR regimen, was associated with worse D30 survival than oral ENR alone (p=0.0002, by pair-wise Mantel-Cox log-rank), suggesting that repetitive handling and trauma entailed by SC administration caused significant toxicity. We therefore explored a curtailed schedule, stopping injections after 14 days (denoted $rBPI_{21}$(14) and VEH(14)). Reasoning that oral antibiotic treatment could be more readily supported in a mass-casualty setting, the ENR schedule was not changed. $rBPI_{21}$(14)/ENR provided the same survival advantage as the longer schedule (Fig. 3B). Six irradiated mice that had

received $rBPI_{21}$(14)/ENR were followed beyond D30, and 5/6 remain alive and healthy appearing at D 131.

Characterization of mitigation regimen effects on GI mucosal mass and plasma levels of inflammatory cytokines early after TBI

Neither $rBPI_{21}$/ENR nor VEH/ENR had a significant effect on the radiation-induced decrease in GI mucosal mass, as reflected by plasma citrulline levels, or its subsequent rapid recovery (Fig. S3). Treatment with ENR, VEH/ENR, or $rBPI_{21}$/ENR had little differential effect on systemic levels of multiple cytokines and chemokines frequently altered early after TBI (Table S2). However, increases in CCL2 and IL-6 concentrations on D6 were significantly greater in $rBPI_{21}$/ENR treated mice (see Discussion).

$rBPI_{21}$/ENR administration mitigates hematopoietic toxicity after TBI

To characterize effects on hematopoiesis, we enumerated bone marrow mononuclear cells retrieved from flushed bone marrow cavities (Fig. 4). At D10, all irradiated groups exhibited fewer bone marrow mononuclear cells than unirradiated, age-matched normals ($p<0.0001$). However, $rBPI_{21}$/ENR treated mice had significantly more bone marrow mononuclear cells than any other irradiated cohort at D10, D15 and D19 (Fig. 4). On D19, $rBPI_{21}$/ENR treated irradiated mice had 80–90% bone marrow cellularity, in contrast to ~20%, <5%, and 10–50%, in the 7 Gy alone, ENR, and VEH/ENR groups, respectively (Fig. 4). Although all surviving mice demonstrated improved cellularity at D30, including the rare survivor of 7 Gy alone, $rBPI_{21}$/ENR treated mice continued to demonstrate greater cellularity (Fig. 5 A–E) and significantly more bone marrow mononuclear cells (Fig. 5F). Trilineage hematopoiesis was observed in all surviving mice (Fig. S4).

Although less than that of unirradiated normals at each timepoint, the absolute number of both LSK and LK cells per hind limb in $rBPI_{21}$/ENR treated mice was significantly greater at both D10 and D19 than observed in other irradiated groups (Fig.6). Only $rBPI_{21}$/ENR treatment was associated with a difference from the untreated, irradiated group. At D30, there was no difference in LSK or LK cell number among surviving mice between treatment groups or between treatment and normal controls.

Bone marrow cellularity changes correlated with changes in peripheral blood counts, which demonstrated rapid and prolonged depression after 7 Gy (Table 1). By D19, $rBPI_{21}$/ENR treated mice demonstrated greater recovery of white blood cell, neutrophil, monocyte and platelet counts than did any other group, and recovery of median white blood cell, neutrophil and monocyte counts to normal levels occurred only in $rBPI_{21}$/ENR treated mice. The white blood cell and neutrophil counts of $rBPI_{21}$/ENR treated mice remained significantly greater than in ENR only treated animals at D30. Equivalent mitigation of hematopoietic toxicity was observed with the shorter $rBPI_{21}$(14)/ENR schedule (Figs. S5, S6).

Discussion

By studying samples from a patient cohort undergoing myeloablative HSCT, we identified molecular and cellular changes potentially related to the toxicity of TBI. The neutropenia that routinely follows myeloablative treatment was associated with rapid depletion of plasma

BPI, a neutrophil-derived protein with potent endotoxin-neutralizing activity (19,21), concurrent with endotoxemia. These changes paralleled cellular (mCD14 and TLR4 surface expression), plasma (IL-6) and physiologic (fever) alterations consistent with increased systemic endotoxin activity (18–20,22,25). We also observed that lower plasma BPI concentrations at the time of HSC infusion correlated with slower myeloid engraftment, suggesting that endotoxin might directly or indirectly exert some negative influence on HSC at time of infusion and for a period thereafter. We therefore explored the hypothesis that exogenous BPI supplementation might mitigate the toxicity of exposure to TBI doses that produce mucosal injury, endotoxemia and prolonged bone marrow aplasia.

We selected $rBPI_{21}$ and a fluoroquinolone antibiotic as components of a mitigation strategy that could be readily actionable; both agents have biologic activity and highly favorable safety profiles in healthy and ill humans, including those with multi-organ compromise (22,26–32). Using an $LD_{95/30}$ single fraction myeloablative TBI model in BALB/c mice, we demonstrated that the $rBPI_{21}$/ENR combination, initiated 24 hours after radiation, was associated with survival rates of 65–80%, significantly greater than the 0–25% observed with VEH/ENR treatment. $rBPI_{21}$ alone did not improve survival. Fluoroquinolones have demonstrated variable efficacy as radiation mitigators, potentially due to differences in experimental design (9,12). In our hands, despite the repetitive injury by $rBPI_{21}$ injection to the irradiated, myeloablated mice, survival after ENR alone treatment was significantly worse, approximately half or less, than observed after $rBPI_{21}$/ENR treatment. Most strikingly, surviving mice on ENR or VEH/ENR treatment demonstrated markedly delayed and inferior hematopoietic recovery than did those treated with $rBPI_{21}$/ENR.

Hematopoietic syndrome contributes significantly to the morbidity and mortality of ARS in humans (2–4,7,33), underscoring the relevance of the observed $rBPI_{21}$/ENR effects on hematopoiesis. Radioprotectants (i.e. agents administered prior to TBI) and potential radiation mitigation strategies generally share some capacity to improve hematologic recovery (2–4,14,15,34–38). However, hematopoietic syndrome mitigation by resourceintensive allogeneic HSCT faces formidable challenges to rapid, successful implementation during a mass radiation exposure (6,7,33), and the efficacy of specific mitigation agents to date has generally been dependent upon administration within minutes to hours after radiation exposure (2–4,12,35–39). Such rapid deployment is unlikely, making strategies that can be delayed for at least 24 hours highly desirable.

There is no established radiation dosimetry technology that can accurately triage exposed individuals and determine those most likely to require mitigation treatment, nor is there a human therapeutic application of TBI without HSC support in which to study the efficacy and toxicity of radiation mitigation agents. These limitations highlight the importance of selecting strategies unlikely to produce toxicity in either minimally affected or critically ill populations. The components of the strategy reported here meet this criterion. Ciprofloxacin, the human-use equivalent of the veterinary fluoroquinolone ENR, was FDA approved in 1987. Fluoroquinolones have excellent oral bioavailability, are well-tolerated (31,32) and have been extensively used after myeloablative chemoradiotherapy. $rBPI_{21}$ is available in a soluble form that is stable stored at 2–8°C, thus facilitating stockpiling. It can be administered SC, IV and intraperitoneally. In addition to showing efficacy in animal models

of pure endotoxemia and Gram-negative bacteremia, $rBPI_{21}$ can abrogate the signs and symptoms of endotoxemia in humans, including associated cytokine dysregulation and coagulopathy (22,29). $rBPI_{21}$ has advantages as an endotoxin neutralizing agent in comparison to anti-endotoxin antibodies whose range and potency is limited (40) and that have, in contrast to $rBPI_{21}$ (28), failed to demonstrate benefit in sepsis studies (41). Moreover, no significant toxicity has been seen in phase 1–3 trials enrolling >1100 normal volunteers and critically-ill patients, including infants and subjects with meningococcemia or undergoing major operative procedures (22,26–30). In aggregate, these data suggest $rBPI_{21}$/ENR could be safely administered to individuals with poorly documented degrees of radiation exposure.

Given the relatively low sensitivity of mice to endotoxin in comparison to humans (19,42), sub-optimal dosing schedule, and relatively greater trauma of repetitive SC injection in mice (readily-accessible ventrolateral body surface area of a human is approximately 100-fold larger than that of an entire mouse), our results may underestimate the potential benefit of this combination treatment. The survival of mice initiating $rBPI_{21}$/ENR treatment 24 hours post-TBI exceeded that observed in similar murine studies, in which mitigators were effective only when initiated 10 minutes-4 hours (16,36,39,43) or up to 20 hours (38) after radiation, and weighs heavily in its favor. Although direct comparison is difficult, our data also suggests $rBPI_{21}$/ENR treatment is associated with earlier and greater improvement in hematopoietic parameters (36,38,39,43). While endotoxin-mediated signaling through TLR4 can alter bone marrow HSC and progenitor numbers and function, with resulting myelosuppression (44), the mechanism underlying the radiation mitigation effect of $rBPI_{21}$/ENR may be multifactorial and extend beyond prevention of endotoxin-induced TLR4 signaling. In that vein, the enhancement of plasma IL-6 concentrations early after initiation of $rBPI_{21}$/ENR treatment is particularly noteworthy, as IL-6 has been shown to contribute to hematopoietic recovery after TBI (45,46). rBPI has been previously shown to reduce IL-6 response to systemic endotoxin when co-administered with purified endotoxin (22,25). Whether this unexpected effect of $rBPI_{21}$ is a consequence of the temporal dissociation between $rBPI_{21}$ administration and onset of endotoxemia, the difference between a radiation versus purified endotoxin challenge, the mitigation of radiation (endotoxin)-induced toxicity to IL-6 producing cells and/or selective inhibition of endotoxin but not other microbial and/or endogenous immune system agonists requires further study. The enhancement of CCL2 levels when treatment of irradiated mice included $rBPI_{21}$ could also contribute to hematopoietic recovery by reducing hematopoietic progenitor cycling (47) and susceptibility to further toxic insults, in a manner postulated to underlie the radiation mitigation activity of PD0332991, a CDK4/6 inhibitor (38). Lastly, the antibacterial activity of $rBPI_{21}$, in combination with a fluoroquinolone antibiotic, might also provide an anti-infective benefit and reduce the potential for emergence of resistant bacterial species in infection-prone, irradiated individuals. Thus, the aggregate effects of this strategy may have potential to limit the scope and duration of supportive care as well as improve survival.

Global concerns about radiation injury consequent to natural disasters, nuclear conflict or terrorism, or as an untoward consequence of intentional medical exposure, have stimulated federal funding that supports development of potential mitigation agents. To date, these have been limited in number and do not yet have optimal characteristics. Given the obligate

overtreatment necessitated by current limitations of radiation dosimetry and the human safety record of $rBPI_{21}$ and fluoroquinolones in critically-ill, myeloablated individuals, the approach outlined here has advantages in comparison to many agents, for which such human data is unlikely to be available prior to a catastrophic event. Moreover, observed efficacy after a delay of 24 hours is particularly important for practical application. Further exploration of this approach, including optimization of the formulation and therapeutic regimen and standardized comparison to other potential mitigators, appears warranted.

Materials and Methods

Patient characteristics

Patients (n=48) undergoing myeloablative allogeneic HSCT from 2005–2009 at Children's Hospital Boston (CHB) or Brigham and Women's Hospital (BWH) were recruited prospectively onto an Institutional Review Board approved study. All participants and/or legal guardians gave consent as appropriate. Patient and treatment characteristics are shown in Table S1. Supportive care was per institutional routine (48,49). Prophylactic oral nonabsorbable antibiotics were administered: bacitracin and polymyxin (BWH) or vancomycin (CHB). Blood counts and cultures were performed in clinical laboratories. Maximal temperature was recorded on the day of sample acquisition ±1 day. Endotoxin Activity Assay measurements, which require fresh samples, could only be performed on patients enrolled after the assay became available.

Blood collection and plasma preparation

Peripheral blood samples were drawn into K2-EDTA or sodium heparin Vacutainer, (Becton-Dickinson) before conditioning (B), on the day of HSCT (D0) and weekly ±1 day, spun at 1200g for 5 min at 4°C, recovered, aliquoted and stored in pyrogen-free tubes at −80°C.

Human BPI and IL-6 ELISA

BPI was measured by ELISA (HyCult), according to the manufacturer's instructions. IL-6 was measured by flow cytometry (MoFlo, DakoCytomation) using antibody-coated fluorescent beads (BD BioSciences) and Summit v4.0 software (DakoCytomation).

Human endotoxin, TLR4 and mCD14 measurements

Endotoxin was measured by Endotoxin Activity Assay according to the manufacturer's instructions (Spectral Diagnostics). Monocyte surface expression of CD14 and TLR4 was measured with antigen-specific or isotype control monoclonal antibodies (eBioSciences) as described (50).

In vivo radiation mitigation studies with $rBPI_{21}$ and enrofloxacin

Male BALB/c mice (Stock # 028, Charles River) were acclimated prior to irradiation at age 12 weeks. Studies were conducted in accordance with Dana-Farber Cancer Institute's ACUC-approved protocols. Mice were placed into a Rad Disk rodent microisolation irradiation cage (Braintree Scientific) and administered a single 7 Gy dose by a Gammacell

40Exactor (Best Theratronics) cesium source irradiator. Twenty-four hours thereafter, mice were either left untreated or received one or more of the following treatments for 14 or 30 days: 1) $rBPI_{21}$, (XOMA), 250 μl per injection of a 2 mg/ml stock constituted in formulation buffer (denoted VEH) and administered SC twice daily, 6–8 hours apart ($rBPI_{21}$/mouse was ~42 mg/kg/day); 2) 250 μl of VEH consisting of 0.33g/L citric acid, 1.01g/L sodium citrate, 8.76g/L sodium chloride, 2.0g/L Poloxamer P188, and 2.0g/L polysorbate 80, (Sigma) dissolved in water for injection, pH adjusted to 5.0, and filter sterilized; 3) Baytril (enrofloxacin, MedVets) at 10 mg/kg/day by gavage via 25G feeding needles (Cadence Science) for the first 5–7 days, after which mice continued to receive antibiotic *ad lib* in water bottles until study termination or death. All mice were observed at least twice daily. Moribund mice were euthanized via CO_2 asphyxiation. At scheduled time points, mice were sacrificed humanely via isoflurane anesthetic overdose (IsoFlo, Abbott Labs).

Blood and Tissue Preparation

Blood counts were determined with a Hemavet 950 FS hematology analyzer (Drew Scientific) with EDTA-anticoagulated (Becton-Dickinson) cardiac blood. Plasma was obtained by mixing blood with pyrogen-free heparin (APP Pharmaceutical), in pyrogen-free Eppendorf tubes (USA Scientific) and centrifugation at 14,000 rpm for 10 minutes. Single-use aliquots were stored at −80°C. In some studies, femurs and tibiae from one leg/animal were dissected, fixed for 24 hours in 10% neutral buffered formalin (Fisher Scientific) and processed, including coronal sectioning and hematoxylin and eosin (H&E) staining (Specialized Histopathology Services-Longwood). Contralateral femurs and tibiae were taken for bone marrow mononuclear cell enumeration and flow cytometry by flushing cells from medullary cavities with cold RPMI 1640 medium supplemented with 10% FBS (JRH Biosciences), L-glutamine, HEPES, pen/strep and gentamicin (all from Invitrogen). Red blood cells were lysed with hypotonic lysing buffer (Sigma). bone marrow mononuclear cell were stained with trypan blue. Dye-excluding viable cells were counted; viability was typically >90–95%.

Citrulline determinations

Samples were analyzed with the MassTrak Amino Acid Analysis system (Waters) with AccQTag(tm) derivatization and ultraviolet/visible detection.

Histopathologic evaluations

A board-certified hematopathologist (JK) assessed femoral bone marrow cellularity on decalcified, formalin-fixed, H&E stained paraffin-fixed sections using an Olympus BX51 microscope, an Olympus DP71 camera and DP Capture software. Two slides with 2 fields/slide were scored per animal for the percent of bone marrow space occupied by hematopoietic cells. A board-certified pathologist (J-AV) enumerated apoptotic bodies/400X field in triplicate samples of H&E-stained paraffin-fixed colon sections. Samples from normal mice were identified, but all others were deidentified and presented for analysis in random order.

Murine endotoxin and cytokine measurements

Endotoxin was measured with the Limulus amoebocyte lysate assay according to the manufacturer's instructions (Charles River). Multi-cytokine analysis was conducted with a commercially-available fluorescent bead-based Luminex® assay (Millipore) per the manufacturer's instructions. Data were acquired on a Bio-Plex 200™ Analyzer (Bio-Rad).

Bone marrow flow cytometry analysis

Bone marrow cells were preincubated with 2% rat anti-mouse CD16/CD32 and 1% normal rat serum for Fc blocking prior to staining cells bearing hematopoietic lineage markers (CD3ε, CD45/B220, CD11b, Ly-6G/Ly-6C, TER 119) with a cocktail of APC-conjugated lineage-specific antibodies, or equivalent concentration of APC-conjugated isotype control immunoglobulins, 1:20 dilutions of PE-rat anti-mouse Sca 1 (clone D7) and PerCP-Cy5.5-rat anti-mouse c-Kit (clone 2B8)(all from Becton-Dickinson). Cells were stained for 25 minutes at 4°C, washed 2× with cold DPBS, and resuspended in 0.4% paraformaldehyde. 100,000 events were acquired on a FACScalibur flow cytometer (Becton-Dickinson) and analyzed with FlowJo v.7.0.5 (Treestar) software. Cells negative for lineage marker expression were assessed for percentages of $Lin^{-}Sca\text{-}1^{-}c\text{-}kit^{+}$ (LK) and $Lin^{-}Sca\text{-}1^{+}c\text{-}kit^{+}$ (LSK) in BONE MARROW (Fig. S7, gating strategy). Data from controls were consistent with published reports in naïve BALB/c mice (51).

Statistics

For the human HSCT study, samples with undetectable analytes were assigned a value at half the lower limit of detection. For ANC, platelet, BPI, TLR4 and IL-6, data were analyzed after logarithmic transformation, which yielded distributions that were more approximately normal. Geometric means and error bars indicating +1 standard error of the mean (SEM) of the log values were then transformed back to original units and plotted on a logarithmic axis. The Wilcoxon signed rank test for matched pairs was employed when comparing values for the same patients at different timepoints, with values compared to baseline. Comparisons between subjects with or without fever were evaluated with the Mann-Whitney test. When assessing correlations between different parameters, within-subject correlations were calculated with the Spearman correlation coefficient and data from multiple timepoints. The calculated coefficients were averaged over the different subjects and significance tested with the signed rank test. All p-values were two-sided. Statistical significance and graphic output were generated with Prism v. 4.0a (GraphPad Software) and SAS v. 9.1 (SAS Institute). Statistical analysis for murine experiments was performed with GraphPad Prism Version 5. Mantel-Cox log-rank was used to compare survival curves. Two tailed Mann-Whitney tests were performed throughout except for PB count and cytokine analyses in which unpaired t tests with Welch's correction for unequal variances were performed. A p value of <0.05 was considered statistically significant. Where indicated in figures, $*p < 0.05$, $**p < 0.01$, $***p < 0.001$.

Supplementary Material

Refer to Web version on PubMed Central for supplementary material.

Acknowledgments

We thank Patrick Scannon, Michael Wessels and Lee Nadler for their insights and support, and Lisa Brennan and Valerie Russo for their many contributions. Supported by: Defense Advanced Research Projects Agency HR001-08-1-0011, NIH 5R21 HL089659 and 5U19 AI067751, the Dana Foundation, the G. Green Foundation and Shea Family Fund.

References and Notes

1. U.S. Department of Health and Human Services. Strategic National Stockpile (SNS) Radiation Emergency Medical Management. 2011 Aug.. http://www.remm.nlm.gov/sns.htm
2. Koenig KL, Goans RE, Hatchett RJ, Mettler FA Jr, Schumacher TA, Noji EK, Jarrett DG. Medical treatment of radiological casualties: current concepts. Ann Emerg Med. 2005; 45:643–652. [PubMed: 15940101]
3. Waselenko JK, MacVittie TJ, Blakely WF, Pesik N, Wiley AL, Dickerson WE, Tsu H, Confer DL, Coleman CN, Seed T, Lowry P, Armitage JO, Dainiak N. Medical management of the acute radiation syndrome: recommendations of the Strategic National Stockpile Radiation Working Group. Ann Intern Med. 2004; 140:1037–1051. [PubMed: 15197022]
4. Stone HB, Moulder JE, Coleman CN, Ang KK, Anscher MS, Barcellos-Hoff MH, Dynan WS, Fike JR, Grdina DJ, Greenberger JS, Hauer-Jensen M, Hill RP, Kolesnick RN, Macvittie TJ, Marks C, McBride WH, Metting N, Pellmar T, Purucker M, Robbins ME, Schiestl RH, Seed TM, Tomaszewski JE, Travis EL, Wallner PE, Wolpert M, Zaharevitz D. Models for evaluating agents intended for the prophylaxis, mitigation and treatment of radiation injuries. Report of an NCI Workshop, December 3–4, 2003. Radiat Res. 2004; 162:711–728. [PubMed: 15548121]
5. Murrain-Hill P, Coleman CN, Hick JL, Redlener I, Weinstock DM, Koerner JF, Black D, Sanders M, Bader JL, Forsha J, Knebel AR. Medical response to a nuclear detonation: creating a playbook for state and local planners and responders. Disaster Med Public Health Prep. 2011; 5(Suppl 1):S89–S97. [PubMed: 21402817]
6. DiCarlo AL, Maher C, Hick JL, Hanfling D, Dainiak N, Chao N, Bader JL, Coleman CN, Weinstock DM. Radiation injury after a nuclear detonation: medical consequences and the need for scarce resources allocation. Disaster Med Public Health Prep. 2011; 5(Suppl 1):S32–S44. [PubMed: 21402810]
7. Baranov A, Gale RP, Guskova A, Piatkin E, Selidovkin G, Muravyova L, Champlin RE, Danilova N, Yevseeva L, Petrosyan L. Bone marrow transplantation after the Chernobyl nuclear accident. N Engl J Med. 1989; 321:205–212. [PubMed: 2664512]
8. Kiang JG, Jiao W, Cary LH, Mog SR, Elliott TB, Pellmar TC, Ledney GD. Wound Trauma Increases Radiation-Induced Mortality by Activation of iNOS Pathway and Elevation of Cytokine Concentrations and Bacterial Infection. Radiation Research. 2010; 173:319–332. [PubMed: 20199217]
9. Brook I, Elliott TB, Ledney GD, Shoemaker MO, Knudson GB. Management of postirradiation infection: lessons learned from animal models. Mil Med. 2004; 169:194–197. [PubMed: 15080238]
10. Packey CD, Ciorba MA. Microbial influences on the small intestinal response to radiation injury. Curr Opin Gastroenterol. 2010; 26:88–94. [PubMed: 20040865]
11. Walker RI, Ledney GD, Galley CB. Aseptic endotoxemia in radiation injury and graft-vs-host disease. Radiat Res. 1975; 62:242–249. [PubMed: 235772]
12. Kim K, Pollard JM, Norris AJ, McDonald JT, Sun Y, Micewicz E, Pettijohn K, Damoiseaux R, Iwamoto KS, Sayre JW, Price BD, Gatti RA, McBride WH. High-throughput screening identifies two classes of antibiotics as radioprotectors: tetracyclines and fluoroquinolones. Clin Cancer Res. 2009; 15:7238–7245. [PubMed: 19920105]
13. Crawford PA, Gordon JI. Microbial regulation of intestinal radiosensitivity. Proc Natl Acad Sci U S A. 2005; 102:13254–13259. [PubMed: 16129828]
14. Ainsworth E. From endotoxins to newer immunomodulators: survival-promoting effects of microbial polysaccharide complexes in irradiated animals. Pharmacology & Therapeutics. 1988; 39:223–241. [PubMed: 3059368]

15. Burdelya LG, Krivokrysenko VI, Tallant TC, Strom E, Gleiberman AS, Gupta D, Kurnasov OV, Fort FL, Osterman AL, Didonato JA, Feinstein E, Gudkov AV. An agonist of toll-like receptor 5 has radioprotective activity in mouse and primate models. Science. 2008; 320:226–230. [PubMed: 18403709]
16. Vijay-Kumar M, Aitken JD, Sanders CJ, Frias A, Sloane VM, Xu J, Neish AS, Rojas M, Gewirtz AT. Flagellin treatment protects against chemicals, bacteria, viruses, and radiation. J Immunol. 2008; 180:8280–8285. [PubMed: 18523294]
17. Roses RE, Xu M, Koski GK, Czerniecki BJ. Radiation therapy and Toll-like receptor signaling: implications for the treatment of cancer. Oncogene. 2008; 27:200–207. [PubMed: 18176601]
18. Beutler B, Rietschel ET. Innate immune sensing and its roots: the story of endotoxin. Nat Rev Immunol. 2003; 3:169–176. [PubMed: 12563300]
19. Munford RS. Sensing gram-negative bacterial lipopolysaccharides: a human disease determinant? Infect Immun. 2008; 76:454–465. [PubMed: 18086818]
20. Diks SH, van Deventer SJ, Peppelenbosch MP. Lipopolysaccharide recognition, internalisation, signalling and other cellular effects. J Endotoxin Res. 2001; 7:335–348. [PubMed: 11753202]
21. Gioannini TL, Weiss JP. Regulation of interactions of Gram-negative bacterial endotoxins with mammalian cells. Immunol Res. 2007; 39:249–260. [PubMed: 17917069]
22. von der Mohlen MA, Kimmings AN, Wedel NI, Mevissen ML, Jansen J, Friedmann N, Lorenz TJ, Nelson BJ, White ML, Bauer R, et al. Inhibition of endotoxin-induced cytokine release and neutrophil activation in humans by use of recombinant bactericidal/permeability-increasing protein. J Infect Dis. 1995; 172:144–151. [PubMed: 7797904]
23. Crenn P, Messing B, Cynober L. Citrulline as a biomarker of intestinal failure due to enterocyte mass reduction. Clin Nutr. 2008; 27:328–339. [PubMed: 18440672]
24. Martinez M, McDermott P, Walker R. Pharmacology of the fluoroquinolones: a perspective for the use in domestic animals. Vet J. 2006; 172:10–28. [PubMed: 16154368]
25. Jin H, Yang R, Marsters S, Ashkenazi A, Bunting S, Marra MN, Scott RW, Baker JB. Protection against endotoxic shock by bactericidal/permeability-increasing protein in rats. J Clin Invest. 1995; 95:1947–1952. [PubMed: 7706502]
26. Bauer RJ, Wedel N, Havrilla N, White M, Cohen A, Carroll SF. Pharmacokinetics of a recombinant modified amino terminal fragment of bactericidal/permeability-increasing protein (rBPI21) in healthy volunteers. J Clin Pharmacol. Pharmacokinetics of a recombinant modified amino terminal fragment of bactericidal/permeability-increasing protein (rBPI21) in healthy volunteers. 1999:1169–1176.
27. Demetriades D, Smith JS, Jacobson LE, Moncure M, Minei J, Nelson BJ, Scannon PJ. Bactericidal/permeability-increasing protein (rBPI21) in patients with hemorrhage due to trauma: results of a multicenter phase II clinical trial. rBPI21 Acute Hemorrhagic Trauma Study Group. J Trauma. 1999; 46:667–676. discussion 76–7. [PubMed: 10217232]
28. Levin M, Quint PA, Goldstein B, Barton P, Bradley JS, Shemie SD, Yeh T, Kim SS, Cafaro DP, Scannon PJ, Giroir BP. Recombinant bactericidal/permeability-increasing protein (rBPI21) as adjunctive treatment for children with severe meningococcal sepsis: a randomised trial. rBPI21 Meningococcal Sepsis Study Group. Lancet. 2000; 356:961–967. [see comment]. [PubMed: 11041396]
29. von der Mohlen MA, van Deventer SJ, Levi M, van den Ende B, Wedel NI, Nelson BJ, Friedmann N, ten Cate JW. Inhibition of endotoxin-induced activation of the coagulation and fibrinolytic pathways using a recombinant endotoxin-binding protein (rBPI23). Blood. 1995; 85:3437–3443. [PubMed: 7780131]
30. Wiezer MJ, Meijer C, Sietses C, Prins HA, Cuesta MA, Beelen RH, Meijer S, van Leeuwen PA. Bactericidal/permeability-increasing protein preserves leukocyte functions after major liver resection. Ann Surg. 2000; 232:208–215. [PubMed: 10903599]
31. Iannini PB. The safety profile of moxifloxacin and other fluoroquinolones in special patient populations. Curr Med Res Opin. 2007; 23:1403–1413. [PubMed: 17559736]
32. Schaad UB. Fluoroquinolone antibiotics in infants and children. Infect Dis Clin North Am. 2005; 19:617–628. [PubMed: 16102652]

33. Dainiak N, Ricks RC. The evolving role of haematopoietic cell transplantation in radiation injury: potentials and limitations. BJR Suppl. 2005; 27:169–174. [PubMed: 15975891]
34. Greenberger JS. Radioprotection. In Vivo. 2009; 23:323–336. [PubMed: 19414422]
35. Herodin F, Drouet M. Cytokine-based treatment of accidentally irradiated victims and new approaches. Exp Hematol. 2005; 33:1071–1080. [PubMed: 16219528]
36. Van der Meeren A, Mouthon MA, Vandamme M, Squiban C, Aigueperse J. Combinations of cytokines promote survival of mice and limit acute radiation damage in concert with amelioration of vascular damage. Radiat Res. 2004; 161:549–559. [PubMed: 15161368]
37. Chen BJ, Deoliveira D, Spasojevic I, Sempowski GD, Jiang C, Owzar K, Wang X, Gesty-Palmer D, Cline JM, Bourland JD, Dugan G, Meadows SK, Daher P, Muramoto G, Chute JP, Chao NJ. Growth hormone mitigates against lethal irradiation and enhances hematologic and immune recovery in mice and nonhuman primates. PLoS One. 2010; 5:e11056. [PubMed: 20585403]
38. Johnson SM, Torrice CD, Bell JF, Monahan KB, Jiang Q, Wang Y, Ramsey MR, Jin J, Wong KK, Su L, Zhou D, Sharpless NE. Mitigation of hematologic radiation toxicity in mice through pharmacological quiescence induced by CDK4/6 inhibition. J Clin Invest. 2010; 120:2528–2536. [PubMed: 20577054]
39. Rwigema JC, Beck B, Wang W, Doemling A, Epperly MW, Shields D, Goff JP, Franicola D, Dixon T, Frantz MC, Wipf P, Tyurina Y, Kagan VE, Wang H, Greenberger JS. Two strategies for the development of mitochondrion-targeted small molecule radiation damage mitigators. Int J Radiat Oncol Biol Phys. 2011; 80:860–868. [PubMed: 21493014]
40. Cross AS. Development of an anti-endotoxin vaccine for sepsis. Subcell Biochem. 2010; 53:285–302. [PubMed: 20593272]
41. McCloskey RV, Straube RC, Sanders C, Smith SM, Smith CR. Treatment of septic shock with human monoclonal antibody HA-1A. A randomized, double-blind, placebo-controlled trial. CHESS Trial Study Group [see comments]. Annals of Internal Medicine. 1994; 121:1–5. [PubMed: 8198341]
42. Warren HS, Fitting C, Hoff E, Adib-Conquy M, Beasley-Topliffe L, Tesini B, Liang X, Valentine C, Hellman J, Hayden D, Cavaillon JM. Resilience to bacterial infection: difference between species could be due to proteins in serum. J Infect Dis. 2010; 201:223–232. [PubMed: 20001600]
43. Chen J, Li C, Guan Y, Kong Q, Li C, Guo X, Chen Q, Jing X, Lv Z, An Y. Protection of mice from lethal Escherichia coli infection by chimeric human bactericidal/permeability-increasing protein and immunoglobulin G1 Fc gene delivery. Antimicrob Agents Chemother. 2007; 51:724–731. [PubMed: 17145792]
44. Rodriguez S, Chora A, Goumnerov B, Mumaw C, Goebel WS, Fernandez L, Baydoun H, HogenEsch H, Dombkowski DM, Karlewicz CA, Rice S, Rahme LG, Carlesso N. Dysfunctional expansion of hematopoietic stem cells and block of myeloid differentiation in lethal sepsis. Blood. 2009; 114:4064–4076. [PubMed: 19696201]
45. Neta R, Perlstein R, Vogel SN, Ledney GD, Abrams J. Role of interleukin 6 (IL-6) in protection from lethal irradiation and in endocrine responses to IL-1 and tumor necrosis factor. J Exp Med. 1992; 175:689–694. [PubMed: 1311016]
46. Sun L, Liu X, Qiu L, Wang J, Liu M, Fu D, Luo Q. Administration of plasmid DNA expressing human interleukin-6 significantly improves thrombocytopoiesis in irradiated mice. Ann Hematol. 2001; 80:567–572. [PubMed: 11732866]
47. Broxmeyer HE, Pelus LM, Kim CH, Hangoc G, Cooper S, Hromas R. Synergistic inhibition in vivo of bone marrow myeloid progenitors by myelosuppressive chemokines and chemokine-accelerated recovery of progenitors after treatment of mice with Ara-C. Exp Hematol. 2006; 34:1069–1077. [PubMed: 16863913]
48. Thornley I, Lehmann LE, Sung L, Holmes C, Spear JM, Brennan L, Vangel M, Bechard LJ, Richardson P, Duggan C, Guinan EC. A multiagent strategy to decrease regimen-related toxicity in children undergoing allogeneic hematopoietic stem cell transplantation. Biol Blood Marrow Transplant. 2004; 10:635–644. [PubMed: 15319775]
49. Armand P, Gannamaneni S, Kim HT, Cutler CS, Ho VT, Koreth J, Alyea EP, LaCasce AS, Jacobsen ED, Fisher DC, Brown JR, Canellos GP, Freedman AS, Soiffer RJ, Antin JH. Improved survival in lymphoma patients receiving sirolimus for graft-versus-host disease prophylaxis after

allogeneic hematopoietic stem-cell transplantation with reduced-intensity conditioning. J Clin Oncol. 2008; 26:5767–5774. [PubMed: 19001324]

50. Levy O, Zarember KA, Roy RM, Cywes C, Godowski PJ, Wessels MR. Selective impairment of TLR-mediated innate immunity in human newborns: neonatal blood plasma reduces monocyte TNF-alpha induction by bacterial lipopeptides, lipopolysaccharide, and imiquimod, but preserves the response to R-848. J Immunol. 2004; 173:4627–4634. [PubMed: 15383597]
51. Zhang P, Welsh DA, Siggins RW 2nd, Bagby GJ, Raasch CE, Happel KI, Nelson S. Acute alcohol intoxication inhibits the lineage- c-kit+ Sca-1+ cell response to Escherichia coli bacteremia. J Immunol. 2009; 182:1568–1576. [PubMed: 19155505]

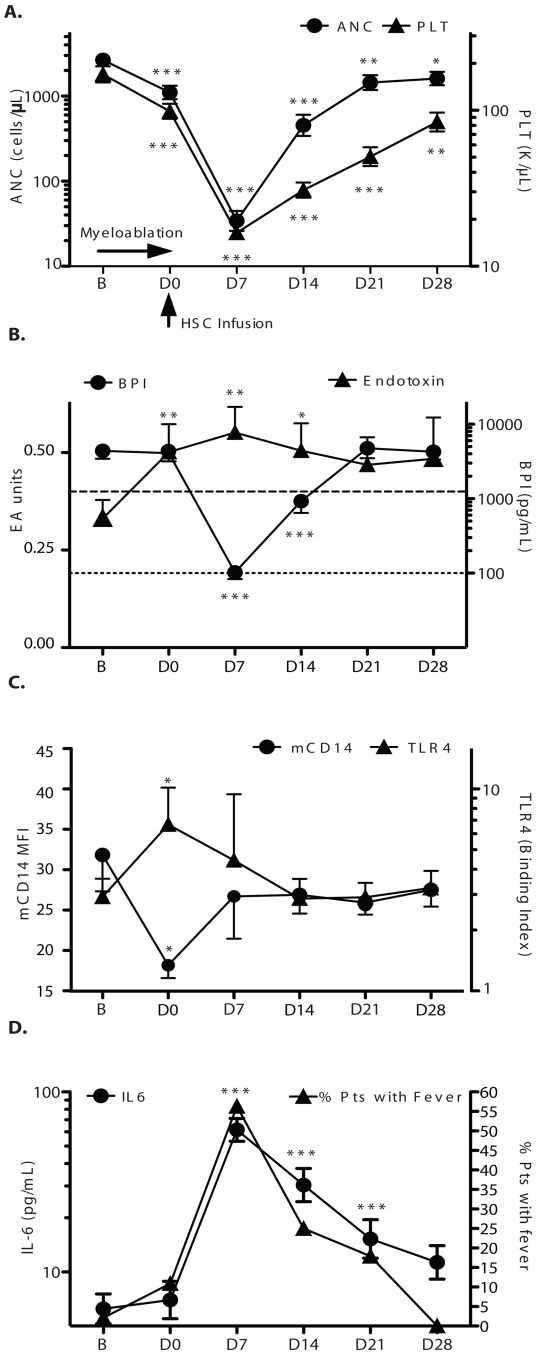

Fig 1.

Changes in peripheral blood counts and endotoxin-related parameters after human myeloablative HSCT. (A) Pattern of neutrophil (ANC) and platelet fall and recovery after myeloablative conditioning treatment. Severe neutropenia (n=46) and thrombocytopenia occurred (n=48, nadir D7). Data represent geometric means ± SEM of log transformed values labeled in original units. (B) Effect of myeloablative HSCT on plasma endotoxin and BPI concentrations. Plasma endotoxin was evaluated in 18 patients by Endotoxin Activity Assay and reported in Endotoxin Activity Assay units at baseline (B; n=17) and for D0

(n=17), D7 (n=10), D14 (n=15), D21 (n=15) and D28 (n=3) after myeloablation. The horizontal dashed line (at 0.4 units) indicates lower limit of detection. Plasma BPI concentrations in pg/mL were assessed by ELISA at B (n=48), D0 (n=46), D7 (n=48), D14 (n=48), D21 (n=47) and D28 (n=33). The dotted line indicates the lower limit of detection for BPI ELISA (<100 pg/ml). Samples below the lower limit of detection were assigned a value of 50% of this limit. (C) Effect of myeloablative HSCT on endotoxin receptor components expressed on monocytes. Monocyte mCD14 and TLR4 surface expression by flow cytometry reached a concurrent nadir for mCD14 (n=10) and peak for TLR4 at D0 (n=9). Data represent mean fluorescence intensity (mCD14) or binding index (TLR4) geometric means ± SEM of log transformed values labeled in original units. (D) Effect of myeloablative HSCT on plasma IL-6 (n=37) and fever (n=48). IL-6 data represent geometric means ± SEM of log transformed values labeled in original units.

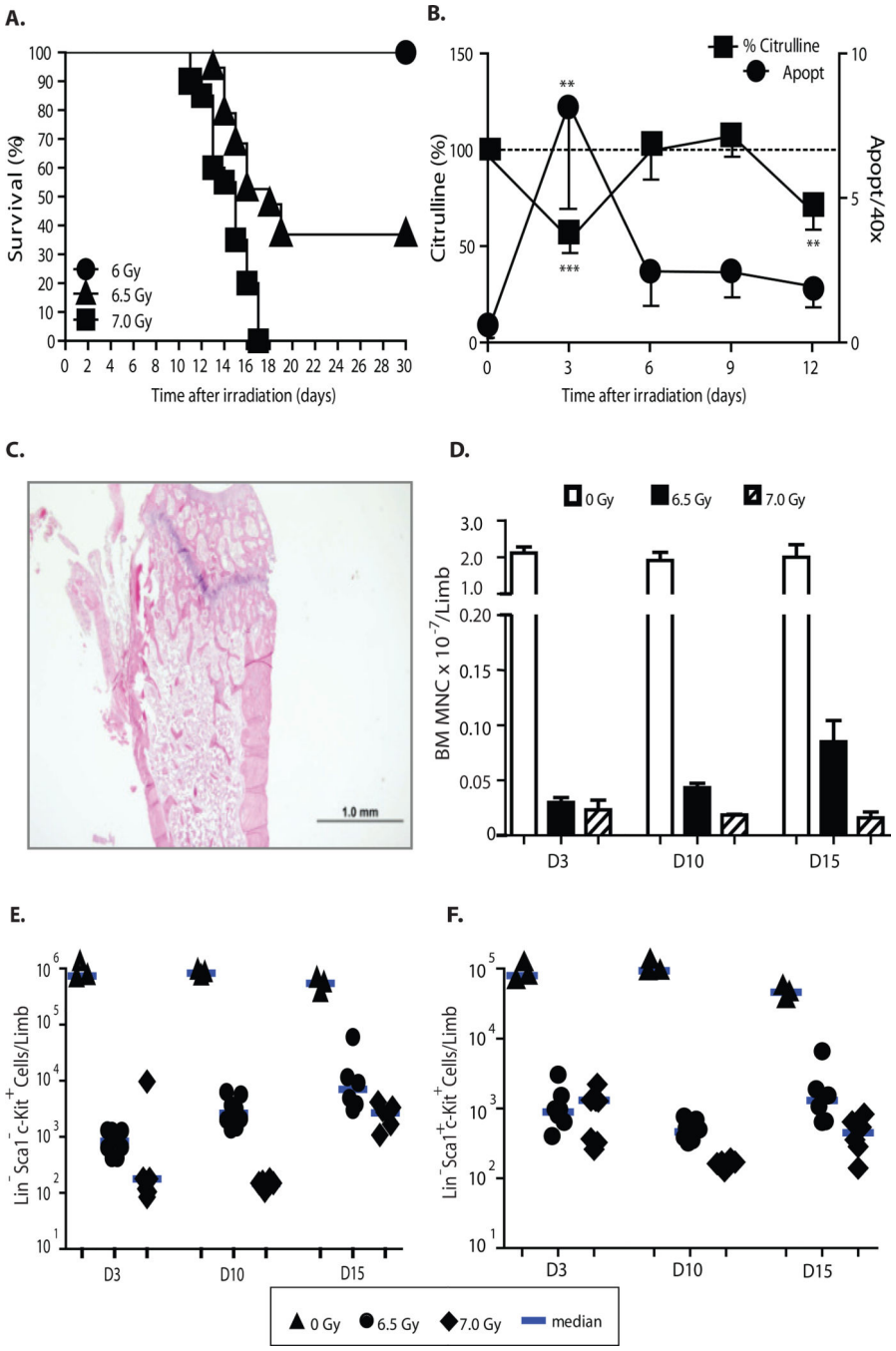

Fig 2.

BALB/c mice exhibit bone marrow ablation and mortality at 7 Gy. (A) D30 mortality after 6 (n=9), 6.5 (n=19) and 7 (n=20) Gy TBI differed by dose ($p<0.001$, Mantel-Cox log-rank). (B) Rapid onset of mucosal damage documented by peak colonic epithelial apoptosis at D3 after TBI (n=5), coincident with nadir in plasma citrulline levels (n=11), depicted normalized to the mean value in unirradiated mice (n=12; D0=100%). Data represent means ± SEM. **$p < 0.01$, ***$p < 0.001$ (comparisons vs. D0). (C) Representative H&E stained femur section demonstrates bone marrow ablation D3 after 7 Gy TBI. Scale bar, 1 mm. (D)

Bone marrow mononuclear cells counted after 0 Gy (normal controls, n=3/timepoint), 6.5 Gy (n= 8/timepoint), and 7 Gy (n= 8 on days 3 and 10, n=6 on D15 due to greater mortality). Data are the mean ± SD of individual counts. Fewer bone marrow mononuclear cells were present after 7 vs 6.5 Gy (D3 p=0.05, D10 p=0.0002, D15 p=0.02) Flow cytometry analysis of LK (E), and LSK cells (F) in bone marrow of the same mice indicated 7 Gy produced prolonged reduction in progenitor and HSC numbers. By D15, 6.5 Gy mice had greater LK and LSK cell numbers than 7 Gy mice (p=0.01 for both LK and LSK). Each symbol represents the absolute LK or LSK number within bone marrow from one limb of an individual animal. Median values are indicated by horizontal bars. Data in panels B, D-F analyzed by Mann-Whitney test.

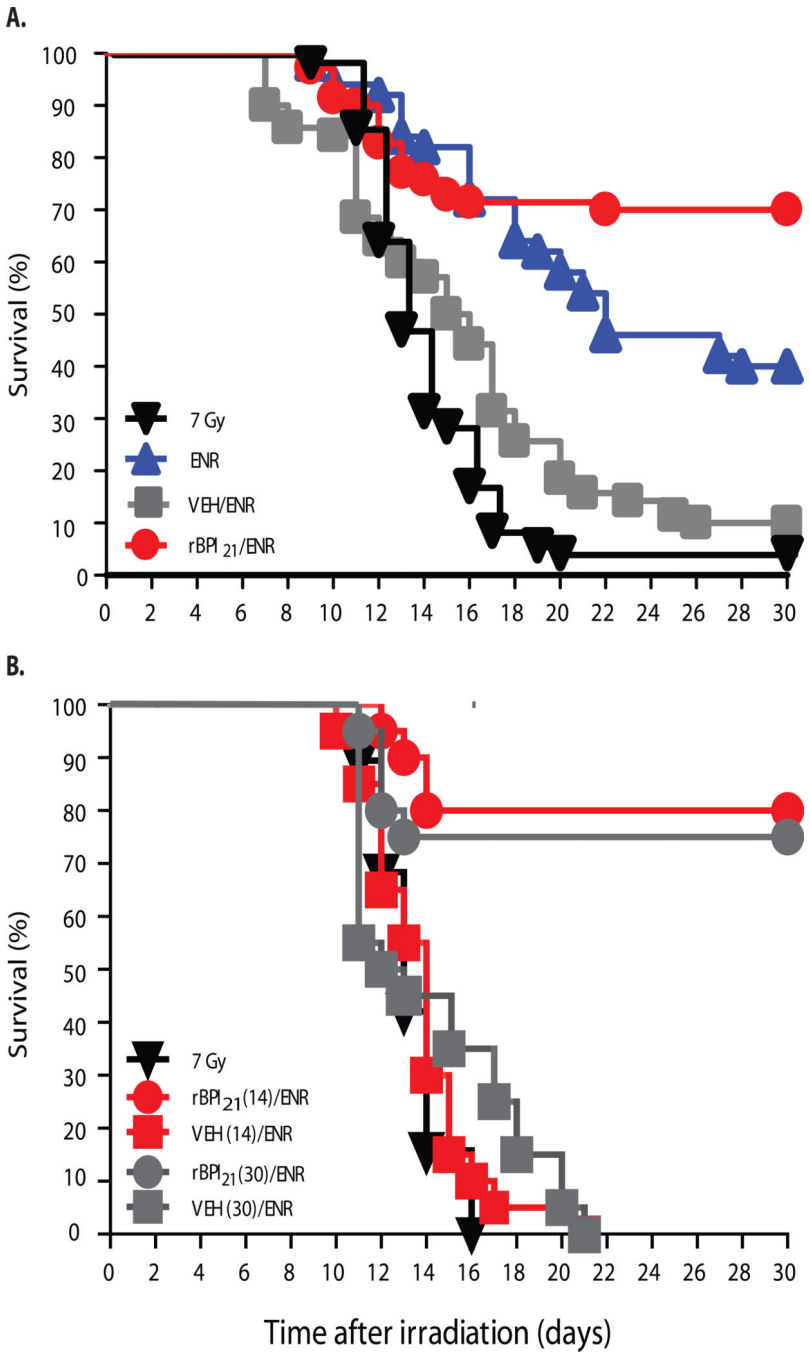

Fig. 3.

$rBPI_{21}$ in combination with ENR enhances survival of BALB/c mice after 7 Gy TBI. (A) Survival of mice initiated on ENR plus $rBPI_{21}$ or VEH, ENR alone, or no treatment (denoted 7 Gy) 24 hours after irradiation and continuing for 30 days. In a composite analysis of 3 replicate experiments, survival of $rBPI_{21}$/ENR treated mice exceeded that of the other groups ($p<0.0001$ by Mantel-Cox log-rank, n=70 mice/arm). Survival of the $rBPI_{21}$/ENR group also exceeded that of VEH/ENR, ENR and 7 Gy ($p<0.0001$, 0.008 and <0.0001, respectively) by pair-wise Mantel-Cox log-rank. (B) Survival of mice initiated on $rBPI_{21}$ or

VEH (continued for either 14 or 30 days) plus ENR (continued for 30 days), or no treatment (denoted 7 Gy) 24 hours after irradiation. Survival was unaffected by duration of $rBPI_{21}$ treatment. Data were analyzed by pairwise Mantel-Cox log-rank, n=20 mice/group.

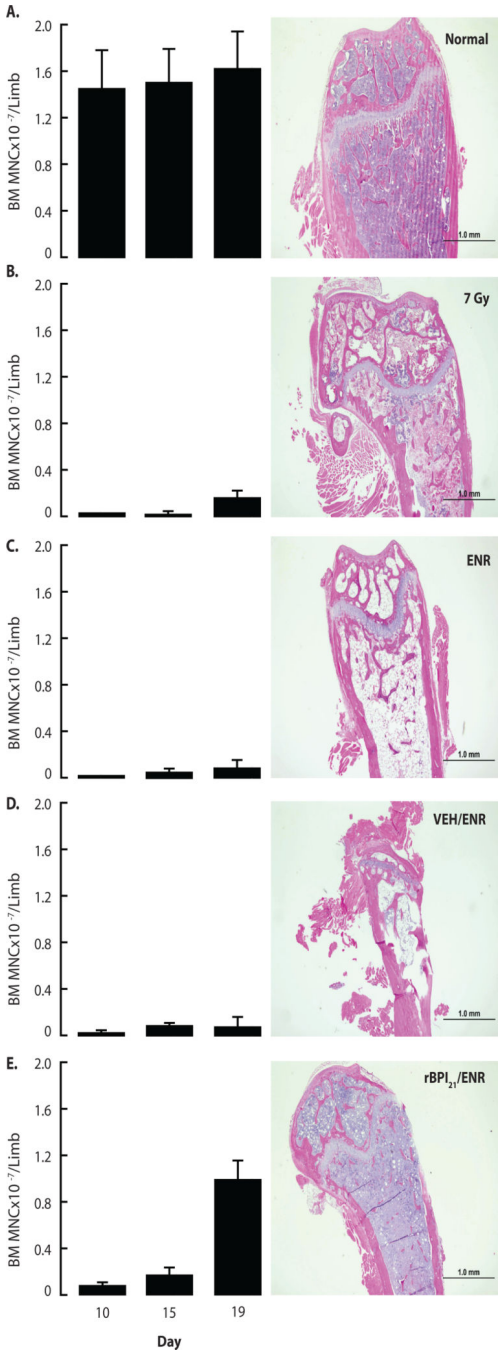

Fig. 4.

rBPI$_{21}$/ENR accelerates hematopoietic recovery after TBI-induced aplasia. BALB/c bone marrow mononuclear cell count (one hind limb) and histopathology (contralateral hind limb) were assessed at D10, D15, and D19. Data shown for (A) untreated, unirradiated age-matched controls (normal) or (B) 7 Gy irradiated mice. Other mice received both 7 Gy TBI and the following treatments started 24 hrs after irradiation: (C) ENR, (D) VEH/ENR or (E) rBPI$_{21}$/ENR. (Left panels) Each graph shows counts (mean ± SD) of bone marrow mononuclear cells flushed from a hind leg of 8 individual mice/group except (B) where

n=2–8/timepoint due to early mortality observed after 7 Gy alone. $rBPI_{21}$/ENR resulted in improved bone marrow cellularity vs. 7Gy, ENR and VEH/ENR on D10 ($p=0.0003$, 0.001 and <0.0001, respectively), D15 ($p=0.0007$, $p=0.001$ and $p=0.001$, respectively) and D19 ($p=0.0006$, $p<0.0001$ and $p<0.0001$, respectively). At each timepoint, all irradiated groups had fewer bone marrow mononuclear cells than controls ($p\leq0.001$). Data analyzed by Mann-Whitney. Data are aggregated from 2 replicate studies. (Right panels) Representative D19 H&E stained femur sections demonstrate the close correlation of bone marrow mononuclear cells counts with bone marrow histology.

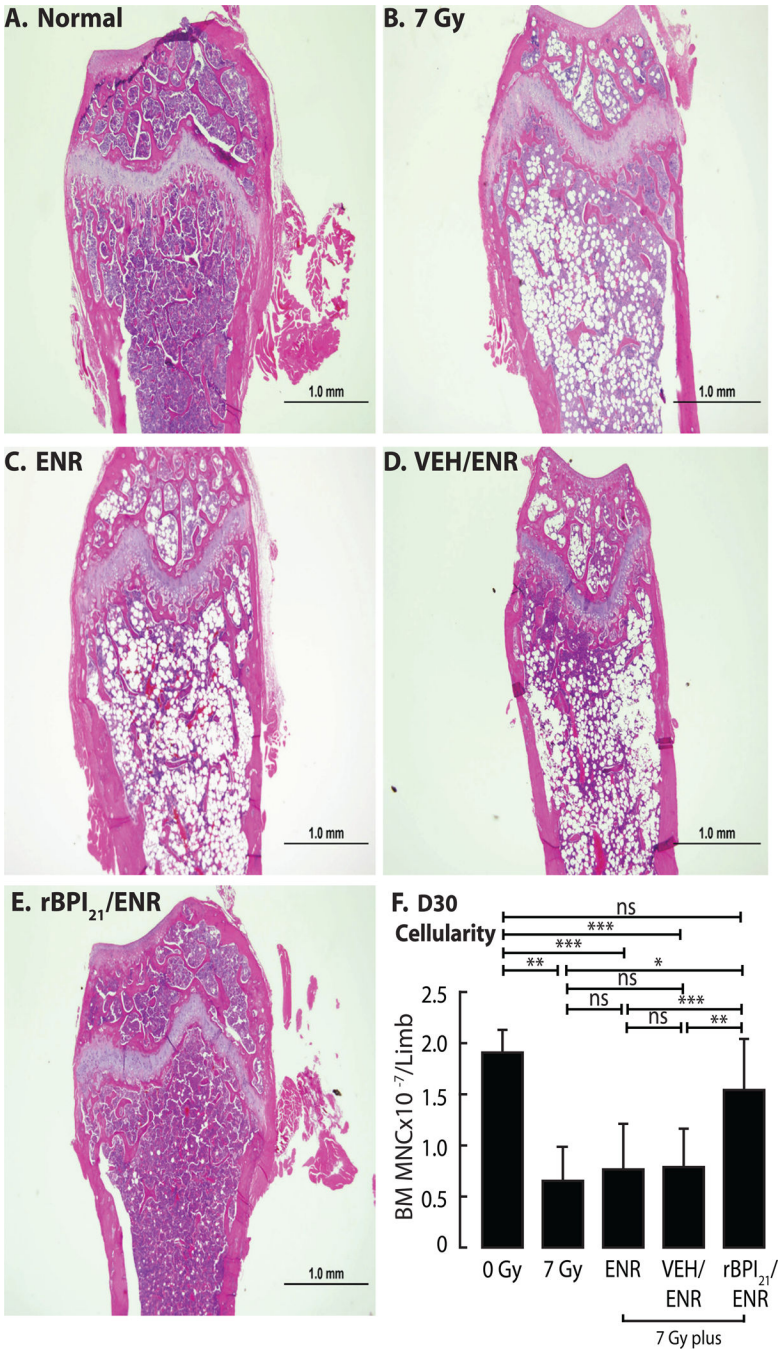

Fig. 5.

rBPI$_{21}$/ENR treatment results in restoration of bone marrow cellularity to normal values by D30 after irradiation. Bone marrow histopathology (one hind limb) and mononuclear cell count (contralateral hind limb) were assessed in mice surviving to D30. Representative femur histology is shown for (A) untreated, age-matched normal or (B) 7 Gy irradiated mice. Other mice received both 7 Gy TBI and the following treatments started 24 hrs after irradiation: (C) ENR, (D) VEH/ENR or (E) rBPI$_{21}$/ENR. In addition to histology, corresponding counts of bone marrow mononuclear cells flushed from a hind leg of

individual mice were determined (F). Bars show mean ± SD for n=4, 3, 12, 7, and 16 mice/group, respectively. The early mortality of 7 Gy alone and VEH/ENR treated mice limited the cohort sizes. Only $rBPI_{21}$/ENR treatment resulted in bone marrow mononuclear cell counts statistically indistinguishable from 0 Gy. $rBPI_{21}$/ENR mononuclear cell counts also differed from counts in 7 Gy, ENR, and VEH/ENR ($p=.01$, $p=0.0002$, $p=0.001$, respectively). Data from 2 replicate studies are shown. Data analyzed by Mann-Whitney.

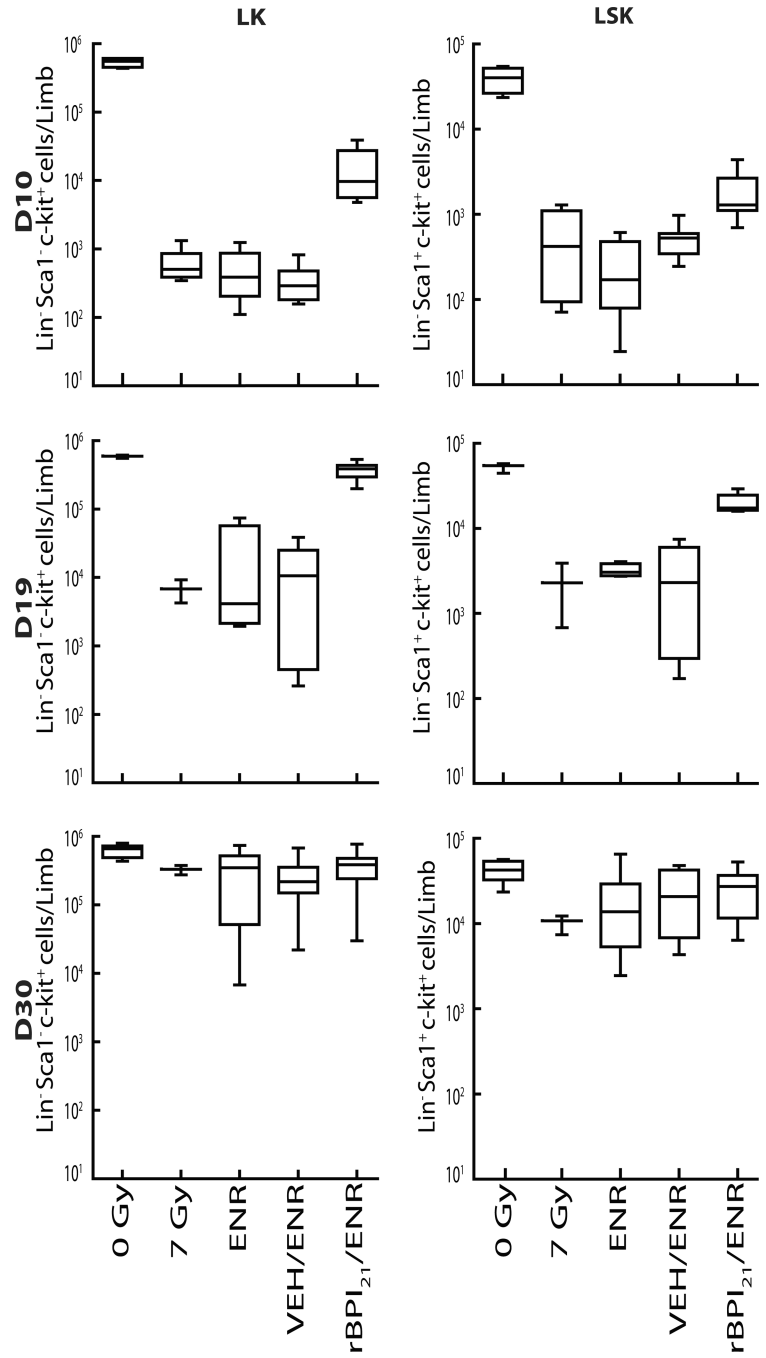

Fig. 6.

$rBPI_{21}$/ENR treatment is associated with more rapid expansion of early hematopoietic cells after 7 Gy TBI. Flow cytometry was used to quantify LK (left panels) and LSK (right panels) cells contained within bone marrow mononuclear cells of age-matched untreated controls (0 Gy) or mice administered 7 Gy and initiated on no treatment (7 Gy), ENR, VEH/ENR or $rBPI_{21}$/ENR treatments 24 hours thereafter. Results from D10, top panels, D19, middle panels, and D30, bottom panels, are shown. Box and whisker graphs depict the range, 25th and 75th percentiles and median number of LK or LSK phenotype cells within

bone marrow from one hind limb of each animal in each treatment group. N=4 for 0 Gy controls at all timepoints. N=8 mice/treatment on D10. N=6–8 mice/treatment at D19. Unequal D30 survival resulted in n=3 (7 Gy), 12 (ENR), 7 (VEH/ENR) and 16 ($rBPI_{21}$/ENR) mice/group. Compared to 7 Gy, ENR or VEH/ENR, $rBPI_{21}$/ENR treatment was associated with greater numbers of LK and LSK cells at early timepoints (p=0.004 for all comparisons on D10 and p=0.004, 0.0003 and 0.0001 on D19, respectively). D30 LK and LSK content of all groups, including normals, was equivalent. Data from 2 replicate experiments are shown. Data analyzed by Mann-Whitney.

Table 1

Peripheral blood counts after TBI by treatment group. Data are shown as median (range). Underlined values indicate the median falls in the normal range of 0 Gy controls.

	White blood cells ($\times 10^{-3}$/μL)	Neutrophils ($\times 10^{-3}$/μL)	Monocytes ($\times 10^{-3}$/μL)	Hemoglobin (g/dL)	Platelets ($\times 10^{-3}$/μL)
0 Gy	4.08 (2.14–11.48)	0.84 (0.46–2.4)	0.24 (0.08–0.37)	15.7 (14.6–17.8)	914 (754–2015)
7 Gy					
D15	0.36 ◆ (0.22–0.38)	0.06 ◆ (0.03–0.08)	0.025 ◆ (0.01–0.04)	10.4 ◆ (8.8–11.3)	195 ◆ (95–225)
D19	0.46 ◆ (0.32–0.61)	0.115 (0.11–0.12)	0.05 ◆ (0.04–0.06)	7.7 ◆ (7.5–7.9)	280.5 ◆ (224–337)
D30	3.98 (2.64–9.68)	1.66 ◆ (1.16–4.86)	0.66 ◆ (0.54–1.58)	13.4 ◆ (13.1–14.3)	692 (680–956)
ENR					
D15	0.24 ◆ (0.14–0.30)	0 ◆●	0 ◆●	8.80 ◆■ (5.6–10.9)	196 ◆ (113–277)
D19	0.21 ◆ (0.18–0.32)	0 ◆●■	0 ◆●■	8.35 ◆■ (6.7–10.9)	250.5 ◆ (185–318)
D30	1.84 ◆● (0.36–4.8)	0.55 ● 0.06–2.34	0.14 ● (0.03–1.03)	13.1 ◆ (2.9–15.5)	713.5 ◆ (128–923)
VEH/ENR					
D15	0.22 ◆ (0.14–0.40)	0.005 ◆ (0–0.09)	0.005 ◆ (0–0.03)	7.1 ◆●◈ (2.4–8.0)	127 ◆ (61–231)
D19	0.38 ◆ (0.28–0.74)	0.07 ◆◈ (0.02–0.18)	0.02 ◆◈ (0.01–0.04)	4.9 ◆●◈ (2.4–7.4)	199 ◆ (95–261)
D30	2.3 (1.42–12.5)	1.05 (0.4–6.31)	0.4 (0.19–3.02)	13.7 ◆ (12.8–14.1)	753 (471–1175)
rBPI$_{21}$/ENR					
D15	0.3 ◆ (0.20–0.32)	0.07 ◆◈ (0.06–0.08)	0.01 ◆ (0–0.02)	7.8 ◆● (6.7–9.4)	229 ◆ (89–254)
D19	2.63 ●◈■ (1.42–7.32)	0.73 ●◈■ (0.29–1.27)	0.26 ●◈■ (0.16–0.62)	10.6 ◆●■ (7.5–11.7)	599.5 ◆●◈■ (360–785)
D30	3.62 ◈ (0.72–5.5)	1.69 ◆◈ (0.15–3.94)	0.44 ◆ (0.07–1.75)	13.7 ◆ (11.0–14.3)	849 (407–1015)

Symbols denote statistical differences: ◆ from 0 Gy; ● from 7 Gy; ◈ from ENR; ■ from VEH/ENR.

All $p<0.05$. Aggregate data from 2 replicate experiments. 0 Gy data pooled from D 15–30, n=11. On D15/19/30, 7 Gy n=5/2/3, ENR n=7/4/12, VEH/ENR n=5/7/7 and rBPI21/ENR n=5/6/13.